Highly Conductive Buried n+ Layers in InP:Fe Created by MeV Energy Si, S, and Si/S Implantation for Application to Microwave Devices

JAYADEV VELLANKI, RAVI K. NADELLA, and MULPURI V. RAO

Department of Electrical and Computer Engineering, George Mason University, Fairfax, VA 22030-4444

To obtain highly conductive buried layers in InP:Fe, MeV energy Si, S, and Si/S implantations are performed at 200°C. The silicon and sulfer implants gave 85 and 100 percent activation, respectively, for a fluence of 8×10^{14} cm^{-2}. The Si/S co-implantation also gave almost 100 percent donor activation for a fluence of 8×10^{14} cm^{-2} of each species. An improved silicon donor activation is observed in the Si/S co-implanted material compared to the material implanted with silicon alone. The peak carrier concentration achieved for the Si/S co-implant is 2×10^{19} cm^{-3}. The lattice damage on the surface side of the profile is effectively removed after rapid thermal annealing. Multiple-energy silicon and sulfur implantations are performed to obtain thick and buried n^+ layers needed for microwave devices and also hyper-abrupt profiles needed for varactor diodes.

Key words: Indium phosphide, implantation, annealing, buried layer

INTRODUCTION

Indium phosphide is emerging as an increasingly important material for microwave and high-power device applications. For these applications, InP can rival or surpass GaAs because of its favorable characteristics (e.g., higher peak electron drift velocity, higher thermal conductivity, lower carrier ionization coefficients, and higher n-type carrier concentration, etc.).[1,2] Microwave devices like varactor diode, mixer diode, and p-i-n diode require thick and buried conductive layers. Either growth techniques or high-energy ion implantation can be used to obtain these buried layers. For these device applications, ion implantation is particularly attractive compared to epitaxial growth because it is more economical, has higher yield, and offers controlled selective area doping, which is not possible with growth technology. Silicon and sulfur are popularly used as dopants to obtain n-type behavior in InP and GaAs.[2–7] Multiple energy implantations of silicon or sulfur species into semi-insulating InP:Fe can be used to create the thick and buried layers mentioned above. It is desirable that these layers be made highly conductive for optimum device performance. For example, the on-state resistance of a p-i-n diode can be decreased by making the buried contact layer highly conductive.[8] High fluence implants ($\geq 10^{15}$ cm^{-2}) need to be used to achieve high conductivity (that is, carrier concentration $\geq 10^{19}$ cm^{-3}). But high fluence implantations lead to amorphization of the material.[9] Once a Group III-V compound material becomes amorphous, it is very difficult to repair the lattice damage and activate the dopant effectively.[7,9] One way of extending the amorphization limits is to perform the implantations at elevated temperatures.[10–12] In InP, silicon predominantly takes indium lattice sites for low implant fluences and acts as a donor. But as the fluence of silicon is increased, its amphoteric nature plays an important role in limiting the maximum net electron concentration that can be achieved.[13–15] To obtain higher electron concentrations than that can be achieved with silicon, either sulfur or co-implantation of sulfur with silicon looks attractive. Because sulfur is not amphoteric, higher carrier concentrations than that with silicon could be obtained, whereas by using Si/S co-implantation, even higher carrier concentrations may be obtained because silicon and sulfur occupy complementary lattice sites to act as donors.

This paper is a report on elevated temperature Si, S, and Si/S implantations into InP:Fe. Wherever appropriate, the results of elevated temperature implants are compared to the corresponding room temperature implant values. We performed 3 MeV Si, 4 MeV S individual implants, and 3 MeV Si/4 MeV S co-implants in InP:Fe for various fluences. As sulfur implantation statistics are not available, we used transport of ions in matter (TRIM) calculations[16] to

(Received May 29, 1992)

find the energy (4 MeV) needed for obtaining overlapping sulfur and silicon carrier profiles. For the silicon ions, for implant energies ≥3 MeV, the implants will be totally buried and the electrical characteristics and lattice quality become almost independent of implantation energy.[7,9,17] Hence, the results presented in this paper are equally valid for ion energies >3 MeV. In this work, we have studied various temperature/time rapid thermal annealing (RTA) cycles to establish the optimum annealing conditions. The as-implanted and the annealed material were characterized by secondary ion mass spectrometry (SIMS), Hall, polaron electrochemical capacitance-voltage (C-V) profiling, and Rutherford backscattering (RBS) techniques to determine the atom concentration depth profiles, sheet carrier concentration, carrier concentration depth profiles, and lattice damage, respectively. To demonstrate the application of elevated temperature high-energy donor implants, we have also performed multiple-energy Si or Si/S implantations into InP:Fe to obtain thick buried layers required for microwave device applications.

EXPERIMENT

Silicon and sulfur implantations were performed into InP:Fe at an elevated temperature of 200°C. The substrates were mounted with a seven degree tilt from the incident beam normal plane and with a 30 degree azimuthal rotation of major flat to minimize channeling. Channeling is more pronounced for the 200°C implantation compared to the room temperature implantation.[10] But the position of the implant peak and the implant distribution on the surface side of the wafer remain the same as for the room temperature implantation.[10] The samples of implanted material were annealed using halogen lamp RTA at various temperatures (800°C to 900°C) for a duration of 10 s. Prior to annealing, a 50 nm thick silicon nitride (Si_3N_4) dielectric cap was deposited on the InP:Fe wafer by plasma enhanced chemical vapor deposition to protect the surface from thermal decomposition during annealing. For additional protection, an InP proximity cap is also placed on top of the Si_3N_4 deposited sample surface during annealing.[18] An AG Associates Heat Pulse 410 annealing station is used for performing the RTAs. The annealing temperature measured by a pyrometer represents the temperature of the silicon wafer sample holder that is in direct contact with the sample to be annealed.

The annealed material is characterized by the van der Pauw-Hall technique for measuring sheet resistance, sheet carrier concentration, and carrier mobility. Electrochemical C-V profiling (polaron) is done to obtain the carrier concentration depth profiles. To correct the error in the polaron profile caused by low InP Schottky barrier height (especially at high carrier concentrations), the profiles are recalibrated by equating the area under the profile to the sheet carrier concentration measured by the Hall technique.[7,10] Implant atom concentration profiles are obtained by secondary ion mass spectrometry. A positive Cesium

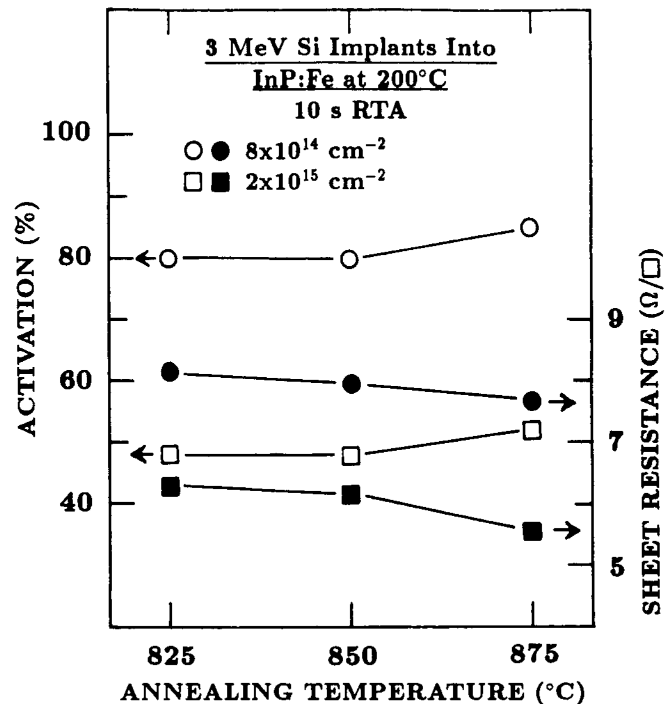

Fig. 1. Percentage of silicon net donor activation and sheet resistance vs. RTA temperature (10 s duration) for 3 MeV silicon implanted InP:Fe at 200°C for fluences of 8×10^{14} and 2×10^{15} cm^{-2}.

beam with 14.5 keV impact energy is used as the primary ion beam. The crystalline lattice quality of the material is determined by RBS measurements. A 4 MeV/He^{++} ion beam is used with a solid state detector placed at an angle of 160 degrees for the backscattered beam.

RESULTS AND DISCUSSION

Figure 1 shows the percentage activation and sheet resistance as functions of RTA temperature for elevated temperature 3 MeV Si implants for fluences of 8×10^{14} and 2×10^{15} cm^{-2}. A 10 s anneal time is used at all temperatures. A maximum dopant electrical activation of 85 percent (52 percent) is obtained for 8×10^{14} (2×10^{15}) cm^{-2} silicon implants at 875°C annealing temperature. This is a substantial improvement over a 45 percent activation achieved for a room temperature (RT) 8×10^{14} cm^{-2} silicon implantation.[7] Even the carrier mobility has improved from the RT implant value of 790 cm^2/V-s to 1,200 cm^2/V-s for the 200°C implant. A detailed room temperature MeV energy silicon implantation results in InP:Fe are given in Ref. 7 and 17. The SIMS measurements on the annealed samples indicated no diffusion of silicon at any annealing temperature. The data in Fig. 1 indicate that the activations are small for higher silicon fluences even if the implants are performed at 200°C. It is clear that, although the elevated temperature implantation is an improvement over room temperature implantation, the maximum net donor (electron) activation (concentration) that can be obtained with silicon implantation is limited by its amphoteric behavior in InP:Fe.[13–15] The peak carrier concentrations obtained for 8×10^{14} and 2×10^{15} cm^{-2} silicon

implants are 9×10^{18} and 1.2×10^{19} cm^{-3}, respectively.[10] Although a carrier concentration of 10^{19} cm^{-3} is sufficient for many device applications, still higher carrier concentrations are desirable for optimum performance in microwave/millimeter wave devices. Hence, to increase the peak carrier concentration further, first we performed sulfur implantation into InP:Fe at 200°C.

Results of RT sulfur implantation in InP:Fe are presented prior to the 200°C implantation results. Room temperature sulfur implants in InP:Fe at 4 MeV gave electrical activations similar to those of RT silicon for fluences $\leq 4 \times 10^{14}$ cm^{-2}.[7] After 875°C/10 s RTA, for a fluence of 4×10^{14} cm^{-2}, we have obtained an electrical activation of 80 percent with a carrier mobility of 1470 cm^2/V-s, whereas, for a fluence of 1×10^{14} cm^{-2}, these values are 100 percent and 1760 cm^2/V-s, respectively. For fluences $>4 \times 10^{14}$ cm^{-2}, a higher donor activation is obtained for RT sulfur implantation compared to RT silicon implantation. For the fluences of 8×10^{14} and 2×10^{15} cm^{-2}, after 875°C/10 s RTA, the dopant electrical activations are 93 and 50 percent and the carrier mobilities are 850 and 660 cm^2/V-s, respectively. The lattice remains severely damaged for these fluences even after annealing.

The plots of percentage activation and sheet resistance versus annealing temperature (10 s duration) for the 4 MeV S implants at 200°C are shown in Fig. 2 for two different fluences. For 8×10^{14} cm^{-2} sulphur, the activation is almost 100 percent at all annealing temperatures, whereas for 2×10^{15} cm^{-2} sulphur, the activation is in the range 82–90 percent. A marginal decrease in the sheet resistance is observed for 2×10^{15} cm^{-2} sulfur with increasing annealing temperature. These values are a clear improvement over the RT values. For the 200°C implant, the SIMS sulfur atom concentration and polaron carrier concentration depth profiles in the as-implanted and annealed samples are shown in Fig. 3 for the 8×10^{14} cm^{-2} fluence. In the SIMS profiles, we have not observed the diffusion of sulfur at any annealing temperature. But a deeper polaron carrier concentration depth profiles with a shoulder are obtained in the annealed samples compared to the SIMS profile. This behavior is not observed for silicon implants. For silicon implants, both silicon SIMS and carrier concentration depth profiles have a close agreement without any diffusion.[10] For sulfur, the formation of a deep shoulder is more pronounced with an increasing annealing temperature. The exact reason for this behavior in sulfur-implanted samples is not known at this time. The peak carrier concentration obtained for 8×10^{14} cm^{-2} fluence of sulfur is 9.6×10^{18} cm^{-3}, whereas for 2×10^{15} cm^{-2} fluence of sulfur, the value we measured is 2×10^{19} cm^{-3}. For the 2×10^{15} cm^{-2} sulfur fluence, the activation seems to be affected by the saturation of phosphorus vacancies by sulfur resulting in a ≤ 90 percent activation.

To obtain still higher peak carrier concentrations than in the case of sulfur, we have performed Si/S co-implantations. The Si/S co-implants are done for fluences of 8×10^{14} cm^{-2} of each species for energies of 4 MeV for sulfur and 3 MeV for silicon. The total electrical activation and sheet resistance results at various RTA temperatures (10 s duration) are shown in Fig. 4. A sheet carrier concentration of 1.6×10^{15} cm^{-2} achieved for 875°C/10 s annealing cycle for a

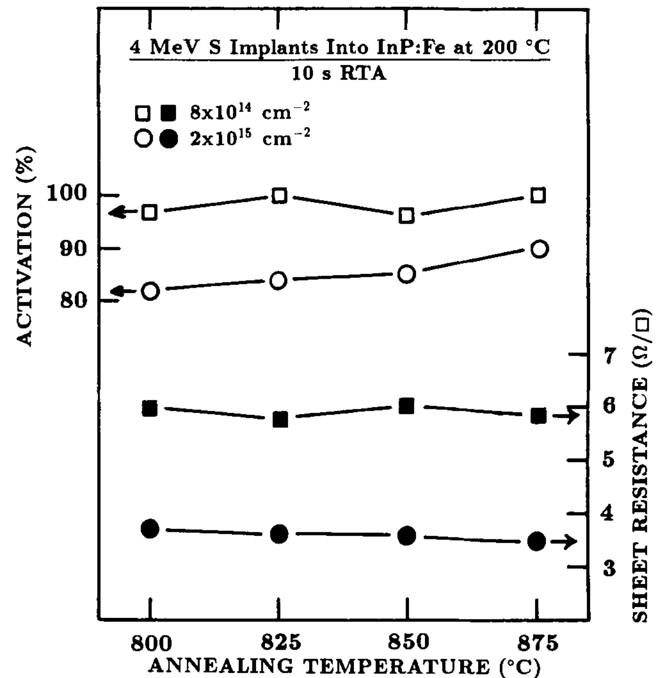

Fig. 2. Percentage of dopant activation and sheet resistance vs. RTA temperature (10 s duration) for 4 MeV sulfur implanted InP:Fe at 200°C for fluences of 8×10^{14} and 2×10^{15} cm^{-2}.

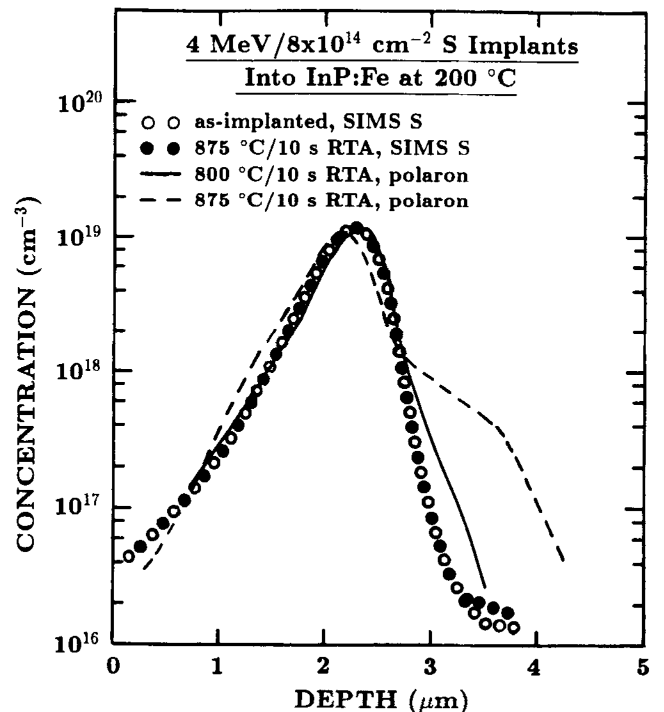

Fig. 3. Secondary ion mass spectrometry sulfur atom concentration and polaron carrier concentration depth profiles in 4 MeV/8×10^{14} cm^{-2} sulfur implanted InP:Fe before and after annealing.

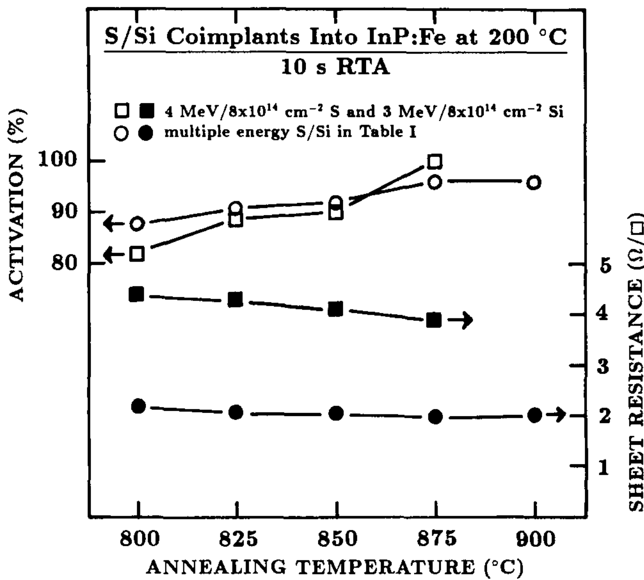

Fig. 4. The total percentage donor activation and sheet resistance vs annealing temperature (10 s duration) for 3 MeV/8 × 10^{14} cm^{-2} silicon and 4 MeV/8 × 10^{14} cm^{-2} sulfur co-implanted InP:Fe at 200°C. The data for a multiple energy Si/S co-implant schedule (Table I) are also included.

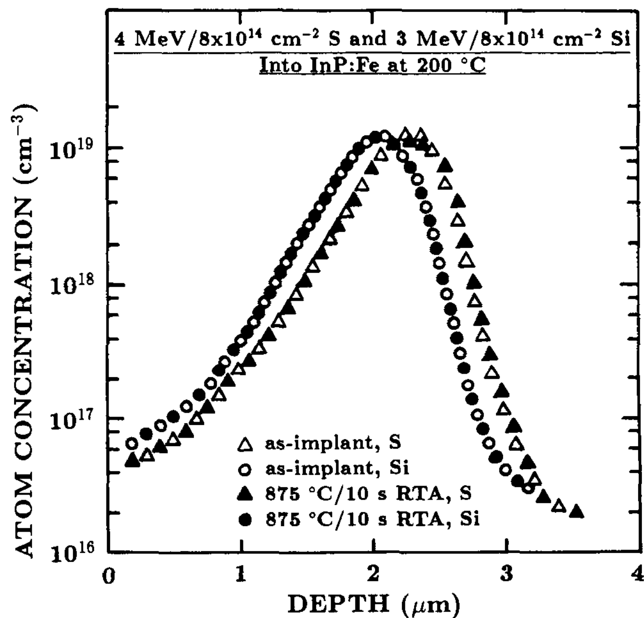

Fig. 5. Secondary ion mass spectrometry silicon and sulfur atom concentration depth profiles in 3 MeV/8 × 10^{14} cm^{-2} silicon and 4 MeV/8 × 10^{14} cm^{-2} sulfur implanted InP:Fe at 200°C before and after 875°C/10s annealing.

fluence of 8 × 10^{14} cm^{-2} for each species (a total Si/S fluence of 1.6 × 10^{15} cm^{-2}) is not the sum of the sheet carrier concentrations obtained for individual 8 × 10^{14} cm^{-2} implants. A clear improvement in silicon activation is achieved for the Si/S co-implant case compared to a value of 85 percent activation for an individual 8 × 10^{14} cm^{-2} silicon implant. This increase of silicon activation in the Si/S co-implant is expected since sulfur is filling the phosphorus lattice sites, thereby reducing the effect of the amphoteric nature of silicon in InP. The mobility and sheet resistance

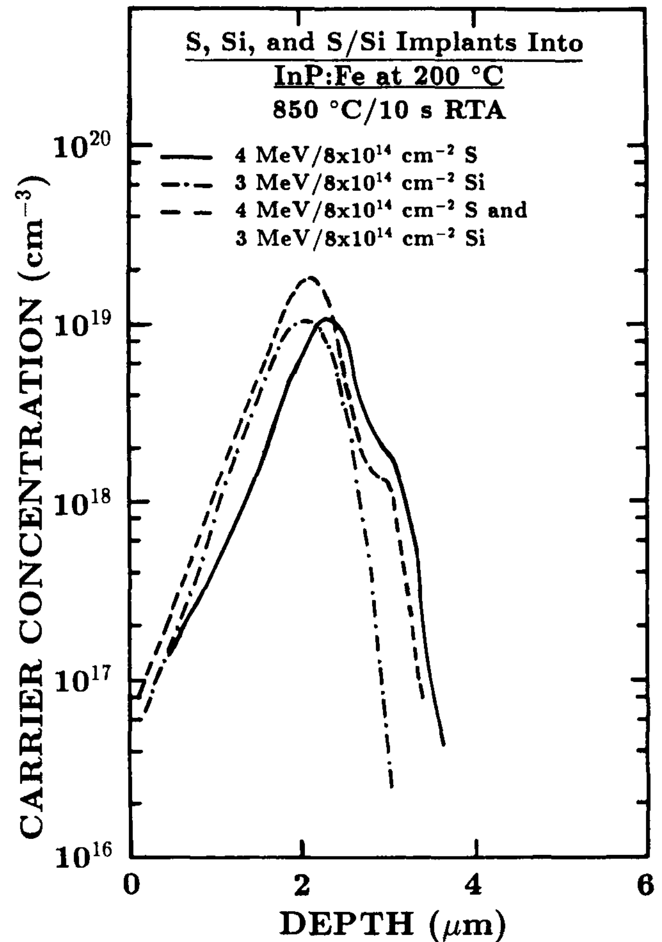

Fig. 6. The polaron carrier concentration depth profiles in Si/S co-implanted and silicon and sulfur individual implanted InP:Fe for 850°C/10 s RTA. The silicon implant is performed at 3 MeV to a fluence of 8 × 10^{14} cm^{-2}, whereas the sulfur implant is performed at 4 MeV to a fluence of 8 × 10^{14} cm^{-2}. All implants were done at 200°C.

corresponding to 100 percent Si/S activation are 1,000 cm^2/V-s, and 3.88 Ω/square, respectively. While a 100 percent donor activation is obtained for the Si/S co-implant, the net donor activation obtained for a comparable fluence (2 × 10^{15} cm^{-2}) silicon implant is 52 per cent while that of sulfur is ≈90 percent.

The atom concentration depth profiles obtained by SIMS measurements before and after annealing for the Si/S co-implanted samples are shown in Fig. 5. The plots are similar for the as-implanted and annealed cases showing little or negligible redistribution of dopant species except for a slight flattening of the peak for sulfur profile. Ideally, the profiles for silicon and sulfur should match exactly to obtain the maximum possible carrier concentration for a given fluence. The mismatch between the profiles is due to the theoretical range statistics that we used for sulfur. These values are obtained from TRIM calculations because of the nonavailability of experimental range statistics for sulfur in InP. For the energies chosen, the amount of overlap between the silicon and sulfur depth profiles is about 80 percent. The polaron carrier concentration depth profile of 4 MeV/8 × 10^{14} cm^{-2} sulfur and 3 MeV/8 × 10^{14} cm^{-2} silicon co-implant is

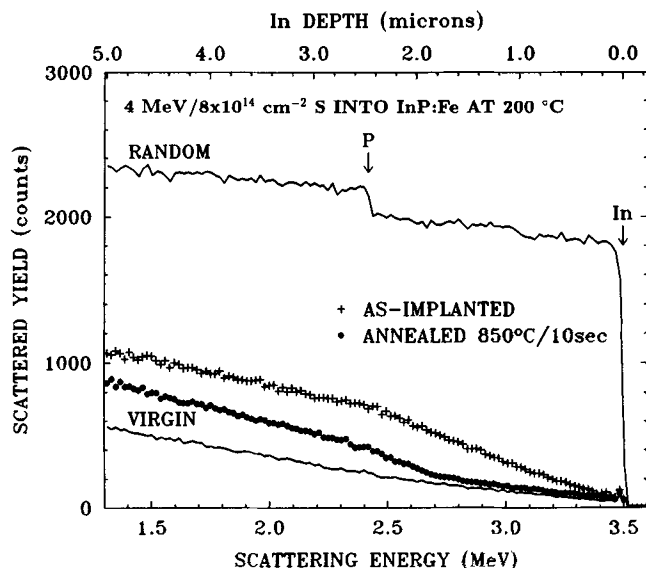

Fig. 7. Rutherford backscattering spectra on 4 MeV/8 × 10^{14} cm^{-2} sulfur implanted InP:Fe before and after annealing.

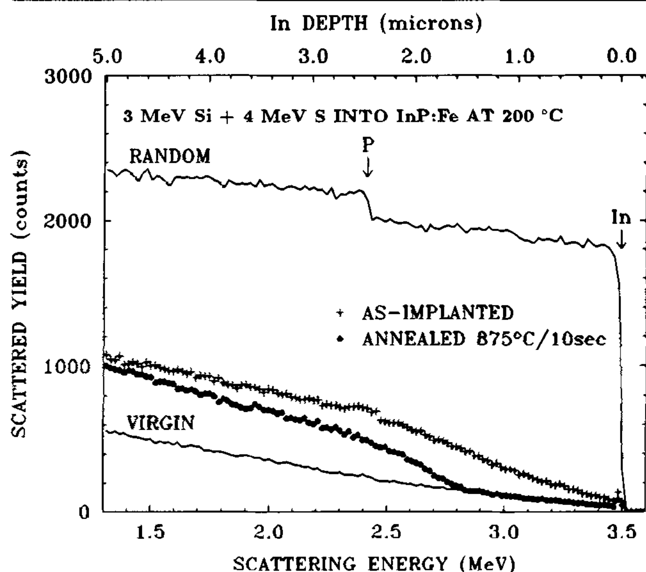

Fig. 8. Rutherford backscattering spectra on 3 MeV/8 × 10^{14} cm^{-2} silicon and 4 MeV/8 × 10^{14} cm^{-2} sulfur co-implanted InP:Fe before and after annealing.

shown in Fig. 6 for 850°C/10 s RTA. For comparison, the profiles for individual implants are also shown in Fig. 6. Peak carrier concentration obtained for the Si/S co-implant is about 2 × 10^{19} cm^{-3}. The peak electron concentrations obtained for InP are almost a decade higher than those for GaAs.[2–4]

The RBS spectra obtained for a qualitative determination of the crystal perfection are shown in Figs. 7 and 8 for S and Si/S implants, respectively. The rise in the yield of the as-implanted spectra from the surface to a depth of 2.4 μm is due to the increasing number of point defects which backscatter the He ion beam away from the channeled direction toward the detector. For both S and Si/S co-implants, the yield of the RBS spectra on the as-implant samples is less than the random yield at all depths indicating that the material is not amorphized at any depth location.

Table I. Multiple Energy Si/S Implantation Schedule Used to Obtain Buried n+ Layer

Specie	Energy (MeV)	Fluence (cm^{-2})
S	7.9	5 × 10^{14}
S	11	5 × 10^{14}
S	15	5 × 10^{14}
Si	6	5 × 10^{14}
Si	8.6	5 × 10^{14}
Si	12	5 × 10^{14}

After annealing for both S and Si/S implants, the RBS yield (up to a depth of ≈1.6–1.8 μm) is close to that of the virgin sample indicating almost complete lattice recovery at these depths. But at depths greater than 1.8 μm, though the yield is smaller than the as-implant yield, it is considerably more than that of the virgin sample. In ion implantation, since the maximum lattice damage is at ≈ $0.8R_p$[19] (which is ≈1.6 μm for 3 MeV silicon) and dislocation loops are formed at ≈$2R_p$, the lattice has not fully recovered at depths ≥1.6 μm. Due to a comparable atom mass of silicon (28.08) and sulfur (32.06), RBS results similar to that of sulfur are obtained for silicon.[10]

Because of the carrier concentration improvement obtained with Si/S co-implantation, we performed multiple-energy Si/S co-implants to obtain highly conductive, thick, and buried layers. The implant schedule used is given in Table I. The Hall measurements for various annealing cycles are shown in Fig. 4. A maximum activation of about 96% is achieved after an annealing cycle of 875°C/10 s. The corresponding mobility, sheet carrier concentration, and sheet resistivity are 1100 cm^2/V-s, 2.88 × 10^{15} cm^{-2}, and 1.97 Ω/square, respectively. The SIMS atom and polaron carrier concentration profiles in this sample are shown in Fig. 9. A 3 μm thick layer with a peak carrier concentration of ≈10^{19} cm^{-3} is achieved. The same shoulder that is observed in the polaron profiles for single energy S and Si/S co-implantation is again observed at a depth of ≈5 μm. By comparing the polaron profile with the sum of silicon and sulfur SIMS depth profiles, we have observed a shift in the polaron profile on the depth scale toward the surface with respect to the SIMS profile. This is due to different techniques used to measure the depth scale in polaron and SIMS.[7] For devices like p-i-n diodes, the buried n+ layer profile has to be at depths greater than that shown in Fig. 9. A similar doping profile at a greater depth can be obtained by using higher ion energies than those given in Table I. For silicon and sulfur, for ion energies ≥3 MeV, the electrical characteristics are almost independent of the ion energy.[7,17]

The RBS spectra for multiple-energy implants is shown in Fig. 10. The as-implanted and annealed spectra are well below the random indicating little lattice damage. However the spectra shows that after a scattering energy of 2.5 MeV, the backscattering yield for the sample annealed by the 875°C/10 s cycle is more than that of the 800°C/10 s annealed sample.

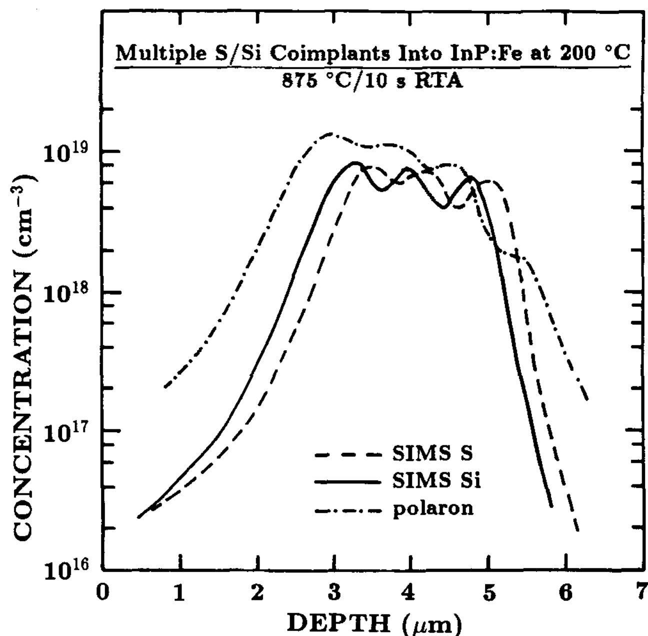

Fig. 9. Secondary ion mass spectrometry silicon and sulfur atom and carrier concentration depth profiles in 875°C/10 s annealed multiple energy Si/S co-implanted InP:Fe. The implant schedule used is given in Table I.

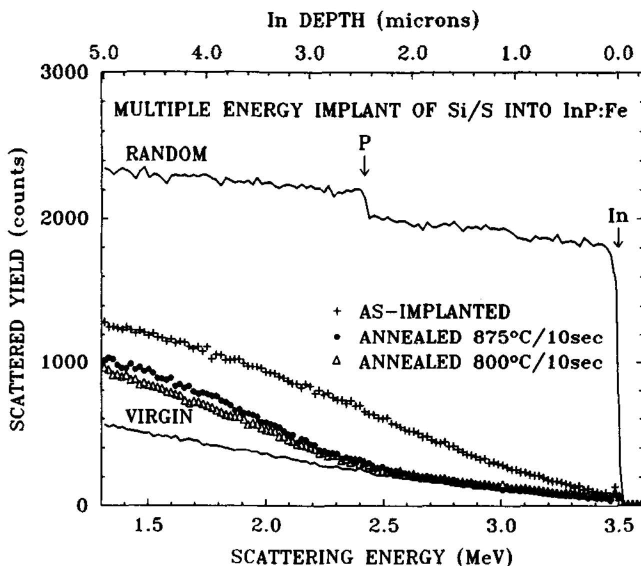

Fig. 10. Rutherford backscattering spectra on multiple energy Si/S co-implanted InP:Fe (implant schedule given in Table I) before and after annealing.

This is probably due to the coalescence of point defects into extended defects[9,10] or the evolution of different defects at the higher annealing temperature. For example, for high fluence implants, a new type of defects called type V defects are formed upon annealing.[20,21] It was proposed that as the impurity moves into substitutional sites, host interstitials are created which form into type V dislocation loops.[21] A similar behavior was also observed by Trudeau et al.[22] for high fluence MeV energy ion implantation in GaAs. Though the yield after 2.5 MeV-scattering energy for the 875°C/10 s RTA is higher than that of 800°C/10 s

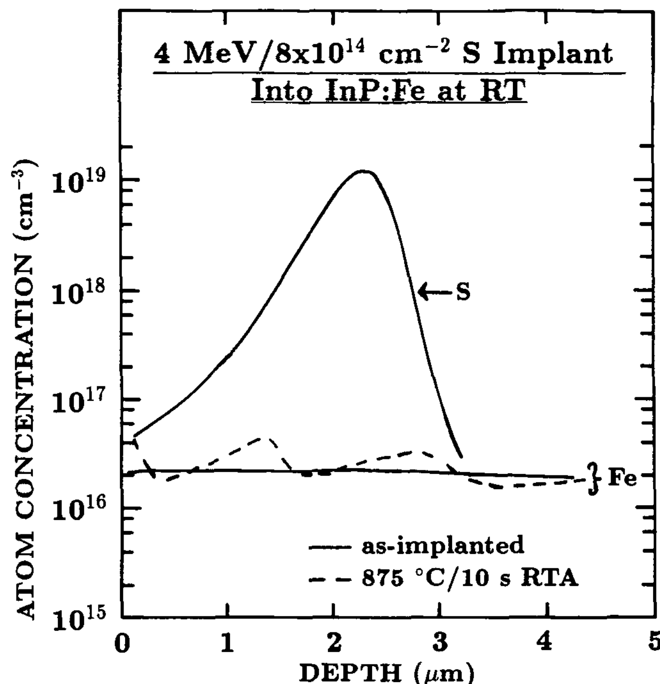

Fig. 11. Smoothed SIMS Fe atom concentration depth profiles in 4 MeV/8 × 10^{14} cm^{-2} sulfur implanted InP:Fe at room temperature before and after annealing. The sulfur SIMS depth profile in the as-implanted material is also shown in the figure.

RTA, it is still close to the virgin level.

A concern of ion implantation into Fe doped semi-insulating InP is the redistribution of Fe during annealing. Transition metals like iron, cobalt, chromium, and vanadium show anomalous diffusion behavior during annealing. To observe this behavior, we have performed SIMS measurements on 4 MeV sulfur as-implanted and annealed material to obtain iron atom concentration depth profiles. These profiles are shown in Fig. 11 for the room temperature implant. In the annealed sample, there is a slight anomalous out-diffusion of iron toward the surface and some re-distribution inside the substrate. Similar iron redistribution behavior was observed by Bahir et al. in silicon implanted InP:Fe.[13] The out-diffusion of iron toward the surface is due to electric field associated with the surface depletion region.[23] The small peaks developed at $\approx 0.7R_p$ and $\approx R_p+\Delta R_p$ of the sulfur implant are due to gettering of iron to the peak implant damage position[19] and the formation of Fe-P complexes in the phosphorus-rich region created by stoichiometric disturbances,[19,24] respectively. The magnitude of iron redistribution is not severe enough to alter the implant carrier concentration depth profiles significantly. For the elevated temperature implants, out-diffusion and redistribution at $\approx R_p+\Delta R_p$ are observed. But the implant-damage-related peak at $\approx 0.7R_p$ is absent due to self-annealing during implantation at 200°C.

Multiple-energy Si, S, and Si/S implantation in InP:Fe is attractive to obtain doping profiles of any shape necessary for microwave devices. For example, for a varactor diode, a hyper-abrupt doping profile is

Table II. Silicon Implantation Schedule Used to Realize Varactor Diode Doping Profile

	Energy (MeV)	Fluence (cm^{-2})
Buried n^+ Implants	12	5×10^{14}
	8.6	5×10^{14}
	6	5×10^{14}
Surface Hyper-Abrupt Doping Profile Implants	1.5	5×10^{12}
	0.75	5×10^{12}
	0.5	7.5×10^{12}
	0.2	1.5×10^{13}

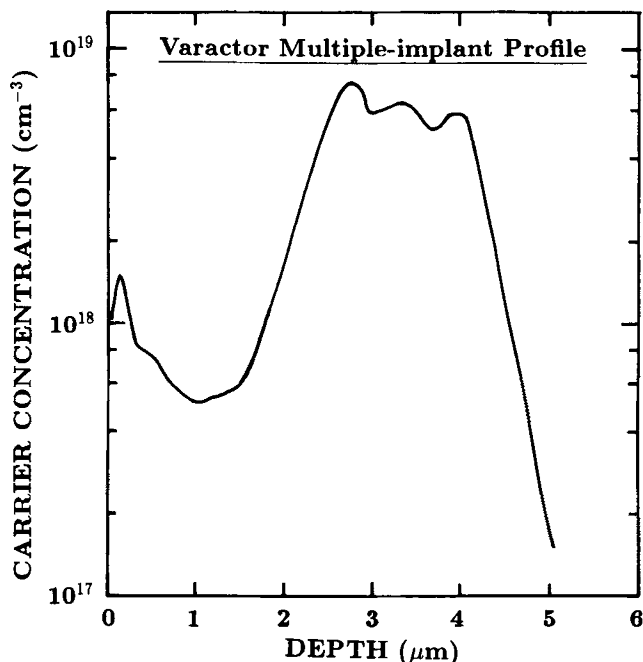

Fig. 12. Polaron carrier concentration depth profile for a multiple energy silicon implantation used (Table II) to make varactor diode in InP:Fe. The implants are performed at 200°C, and the annealing cycle used is 875°C/10 s RTA.

required at the surface (to obtain a linear voltage variable capacitance relation) and a thick highly conductive buried n^+ ohmic contact region is required in the bulk.[25] A typical silicon multiple implant schedule used to obtain both hyper-abrupt and buried n^+ layers is given in Table II. All implants are performed at 200°C. The polaron carrier concentration depth profile in the sample annealed by 875°C/10 s RTA is shown in Fig. 12. This profile demonstrates the versatility of high energy implantation to make microwave devices that require doping profiles of any shape. To obtain optimum performance, multiple-energy Si/S co-implantation instead of multiple-energy silicon implants should be used for the buried n^+ layer, whereas for the hyper-abrupt layer, only silicon implants suffice because the required silicon implant fluences to create this layer are low for which the activation is almost 100 percent. In fact, for the hyper-abrupt layer, even room temperature implants can be used because, for the fluences used, the as-implant damage RBS yield is much below the random level and hence can be easily annealed.

CONCLUSIONS

Buried n^+ layers with a maximum carrier (electron) concentration of 10^{19} cm^{-3} can be obtained with 200°C MeV Si implantation in InP. To obtain electron carrier concentrations $>10^{19}$ cm^{-3} in InP, elevated temperature S implantation or Si/S co-implantation seem to be more effective than Si implantation. For high silicon fluences, due to the amphoteric nature of silicon, some of silicon takes phosphorus sites resulting in poor net donor activation. Since sulfur is not an amphoteric impurity, this problem does not exist but the maximum possible electron concentration is still limited by the saturation of phosphorus vacancies by sulfur. Instead of high fluence Si or S, if Si/S co-implant of equal total fluence is used, a higher electron concentration can be obtained. This is because In and P lattice sites can be filled by silicon and sulfur, respectively, to obtain donors. Since phosphorus sites are occupied by sulfur, the amphoteric behavior of silicon is also suppressed by Si/S co-implantation. Since the implant damage on the surface side of the profile is effectively removed, high fluence Si, S, or Si/S implants are attractive for making buried high carrier concentration n^+ layers, required for microwave devices like p-i-n diode, varactor diode, etc. Multiple-energy silicon and sulfur implantations in InP:Fe are very useful for obtaining doping profiles of any shape for the above device applications. In this study, by using elevated temperature S and Si/S implantations in InP:Fe, we have obtained buried layers with a maximum carrier concentration of 2×10^{19} cm^{-3}. To obtain the overlap of sulfur and silicon implant profiles accurately, we are currently developing the range statistics of sulfur ions in InP up to 16 MeV energy using the SIMS sulfur atom concentration depth profile measurements. For sulfur implants, the polaron carrier concentration depth profiles show a shoulder at depths greater than the implant depth. The reason for this behavior is not known at this time. No diffusion of sulfur is observed in the SIMS measurements performed on the annealed samples at any annealing temperature. The 875°C/10 s RTA cycle seems to be the optimum annealing condition for all high fluence implants used in this study.

ACKNOWLEDGMENT

The authors are grateful to H.B. Dietrich, B. Molnar, N. Papanicolaou, and W. Moore of the Naval Research Lab, O.W. Holland of Oak Ridge National Laboratory, D.S. Simons, and P.H. Chi of the National Institute of Standards and Technology for their help during the course of this study. This paper is based upon work supported by the National Science Foundation under Grant #ECS-9022438.

REFERENCES

1. B. Fank, *Microwave J.* 27, 95 (1984).
2. D.E. Davies, J.P. Lorenzo and T.G. Ryan, *Solid-State Elec-*

tron. 21, 981 (1978).

3. R G. Wilson, D.M. Jamba, V.R. Deline, C.A. Evans, Jr. and Y.S. Park, *J. Appl. Phys.* 54, 3849 (1983).
4. S.S. Chan, B.G. Streetman and J.E. Baker, *J. Electrochem. Soc.* 132, 2467 (1985).
5. P.E. Thompson and H.B. Dietrich, *J. Electrochem. Soc.* 135, 1240 (1988).
6. P.E. Thompson, *Nucl. Instrum. Methods* B59/60, 592 (1991).
7. R.K. Nadella, M.V. Rao, D.S. Simons, P.H. Chi, M. Fatemi and H.B. Dietrich, *J. Appl. Phys.* 70, 1750 (1991).
8. R.K. Nadella, J. Vellanki, M.V. Rao and H.B. Dietrich *IEEE Electron Dev. Lett.* 13, 473 (1992).
9. S.M. Gulwadi, R.K. Nadella, O.W. Holland and M.V. Rao, *J. Electron. Mater.* 20, 615 (1991).
10. M.V. Rao, R.K. Nadella and O.W. Holland, *J. Appl. Phys.* 71, 126 (1992).
11. J.P. Donnelly, *Nucl. Instrum. Methods* 182, 553 (1981).
12. K. Gamo, M. Taki, H. Yagita, N. Takada, K. Masuda, S. Namba and A. Mizobuchi, *J. Vac. Soc. Technol.* 15, 1086 (1978).
13. G. Bahir, J.L. Merz, J.R. Abelson and T.W. Sigmon, *J. Appl. Phys.* 65, 1009 (1989).
14. A. Dodabalapur and B.G. Streetman, *Ion Implantation and Dielectrics for Elemental and Compound Semiconductors,* ed. S.J. Pearton, K.S. Jones and V.J. Kapoor (Pennington, NJ: Electrochemical Society, 1990), p. 66.
15. M.C. Ridgway, C. Jagadeesh, T.D. Thompson and S.T. Johnson, *J. Appl. Phys.* 71, 1010 (1992).
16. J.F. Ziegler, J.P. Biersack, and U. Littmark, *The Stopping and Ranges of Ions in Solids* (New York: Pergamon, 1985).
17. R.K. Nadella, M.V. Rao, D.S. Simons, P.H. Chi and H.B. Dietrich *J. Appl. Phys.* 70, 7188 (1991).
18. M.V. Rao and P.E. Thompson, *Appl. Phys. Lett.* 50, 1444 (1987).
19. L.A. Christel and J.F. Gibbons, *J. Appl. Phys.* 52, 5050 (1981).
20. K.S. Jones, E.L. Allen, H.G. Robinson, D.A. Stevenson, M.D. Deal and J.D. Plummer, *J. Appl. Phys.* 70, 6790 (1991).
21. K.S. Jones, M. Bolling, T.E. Haynes, M.D. Deal, E.L. Allen and H.G. Robinson, *Mat. Res. Soc. Symp. Proc.* 240, 785 (1992).
22. Y.B. Trudeau, G.E. Kajrys, G. Gagnon and J. L. Brebner, *Nucl. Instr. and Meth. in Phys. Res.* B 59/60, 609 (1991).
23. M. Ganneau, R. Chaplain, A. Rupert, E.V.K. Rao and N. Duhamel, *J. Appl. Phys.* 57, 1029 (1985).
24. S. Nakahara, S.N.G. Chu, J.A. Long, V.G. Riggs and W.D. Johnson, Jr., *J. Cryst. Growth* 68, 693 (1984).
25. P.J. McNally, T.Smith, F.R. Phelleps, K.M. Hogan, B. Smith and H.B. Dietrich, IEEE MTT Intl. Symp., 1990, Dallas, TX.